Pergamon

NanoStructured Materials, Vol. 5, Nos. 7/8, pp. 745–754, 1995
Elsevier Science Ltd

0965-9773/95 $9.50 + .00

0965-9773(95)00291-X

THEORETICAL INVESTIGATION OF THE THERMODYNAMIC STABILITY OF NANOSCALE SYSTEMS—III: THIN FILM WITH AN IPB

Ryoichi Kikuchi* and **Long-Qing Chen****

*Department of Material Science and Engineering, University of California at Los Angeles, Los Angeles, CA 90095-1595, USA
**Department of Materials Science and Engineering, Pennsylvania State University, University Park, PA 16802, USA

(Accepted August 1995)

Abstract—*Thermodynamic stability of nanoscale thin films is analyzed theoretically using equilibrium statistical mechanics. A model binary system with a miscibility gap is treated in fcc using the pair approximation of the Cluster Variation Method. Each film has equal total numbers of A and B atoms, and has an interphase boundary (IPB) around the center of a film at low temperatures. The composition profile across the film is calculated for different temperatures and thicknesses. The result reveals that the composition inside a film is practically the same as that of the corresponding bulk fcc system, and the surface composition is close to that of the two-dimensional surface lattice. For a fixed temperature, the mutual solubility of two components increase as the film thickness decreases, and becomes totally miscible for very thin films. For a given thickness, the miscibility increases with the temperature, and the critical temperature T_c of phase separation is determined as a function of film thickness.*

INTRODUCTION

In Paper I of this series (1) we studied thermodynamic stability of a nanoscale layer structure of a phase-separating binary alloy. The layers are repeated periodically, and hence the structure is theoretically infinitely thick. We calculated the composition profile for different temperatures and different layer thicknesses, and showed how the phase-separating temperature depends on the unit layer thickness. The present paper examines the similar physical properties on a thin film of finite thickness containing one interphase boundary. The main feature of the present study of finite thickness films is the surface effect, which was not present in Paper I, and cannot be ignored in real systems.

As was done in Papers I and II (2), the model we work on is an A-B alloy without vacancies on an fcc lattice with a repulsive effective interaction between A and B atoms. We assume the composition of 50 atomic percent each, and hence the problem is mathematically equivalent to the Ising model. We choose the boundary conditions of the film in such a way that on one surface of

the film the structure is A-rich while on the other surface B-rich, and the boundary between the two phases, which is called the interphase boundary (IPB), exists around the center of the film. The calculation is done using the pair approximation of the Cluster Variation Method (CVM) (3), as was done in Paper I. Although the system is fcc, the pair approximation is qualitatively reliable since no sublattice structure occurs.

It is worth noting the restrictions of the model we work with. The first is that relaxation of the lattice near the surface and near the junction is neglected. The relaxation is due either to segregation of vacancies or to the local change of the lattice constant. The vacancy effect can be taken into account in the same framework as the present paper, but we have not done it. To take into account the lattice constant relaxation effect is left as the future challenge to the continuous displacement treatment recently being developed (4,5). The second restriction is that the spinodal decomposition within the plane parallel to the junction is neglected. The paper is only concerned about giving the phase boundary information.

A related work was reported by a Mexican group (6) using a similar CVM treatment. Their main interest was the magnetic effect.

CVM FORMULATION OF A FILM WITH FREE SURFACES

Different from Paper I, the film has two free surfaces, and hence needs a special care to treat the region near the surfaces, although most of the formulation remains the same as I. The layer is placed in the [100] orientation. Different from I, this paper uses the position coordinate m different from the numbering of lattice planes n. The position for a plane n is at m = 2n. This is done in order to make the bond positions between two planes by odd numbers, m = 2n+1 as shown in Figure 1.

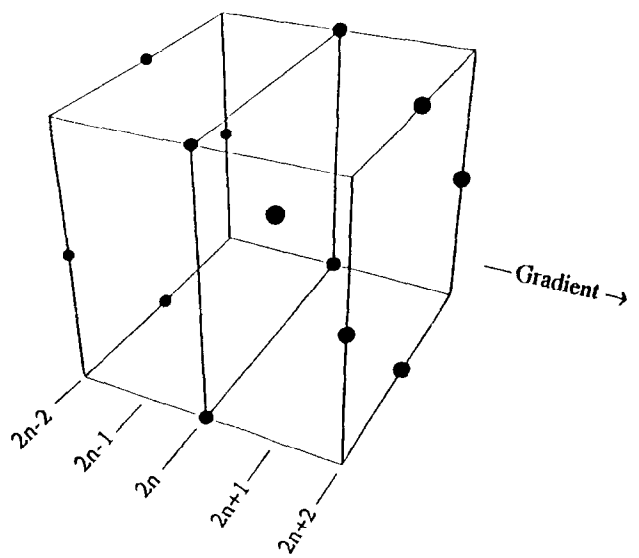

Figure 1. The gradient direction, the lattice plane number 2n and the bond number 2n+1.

When we assume the symmetric geometry across the thickness, we classify two cases, one with an even number of planes and the other odd. In the even number case, the center of the IPB is between two planes, and we call this the *interstitial center* case (7) for short. In the odd number thickness case, we have the *atomic center* IPB (7). As an illustration of the formulation, we report equations for the even number of planes with the interstitial IPB. We call the total number of planes in the film the *thickness* and write it as n_h. The positions of the lattice planes are from m = 2 to $2n_h$ in units of the lattice constant. The center of the IPB is at the bond position $m = n_h+1$, between the lattice planes at $m = n_h$ and n_h+1.

We write the point probability variables at m = 2n as x(i;2n), where i = 1 and 2 for A and B species, respectively. Since each lattice point has nearest neighbors within the same plane and in neighboring planes, we have two kinds of pair variables. Those inside a lattice plane are written as $y_n(ij;2n)$, and those connecting two neighboring planes as $y_u(ij;2n+1)$. The subscript n in y_n stands for "normal" and has no relation to the plane number n.

The steps of the formulation are essentially the same as those in Paper I. We need several modifications. The first modification is on the constraint relations, which are written for inside points and for end points separately.

For inside points from n=2 through n_h-2,

$$x(i;2n) = \sum_j y_u(ji;2n-1) = \sum_j y_u(ij;2n+1) \qquad [1.a]$$

$$x(i;2n) = \frac{1}{2}\left(\sum_j y_u(ji;2n-1) + \sum_j y_u(ij;2n+1)\right) = \sum_j y_n(ij;2n) \qquad [1.b]$$

For end points

$$\text{At n=1,} \quad x(1;m=2) = \sum_j y_u(ij;3) = \sum_j y_n(ij;2) \qquad [2.a]$$

$$\text{At n=n}_h, \quad x(1;m=2n_h) = \sum_j y_u(ji;2n_h-1) = \sum_j y_n(ij;2n_h) \qquad [2.b]$$

In addition to these constraint equations, we need the normalization for y's for each location. The constraints are treated using Lagrange multipliers.

The second modification is for the entropy expression. When we construct the entropy using the concept of the correlation correction factor, which was introduced and discussed in detail in a recent publication (8), it is derived on an ensemble as follows. k_B is the Boltzmann constant.

$$\exp\left(\frac{S}{k_B}\right) = \prod_{n=1}^{n_h} W(2n)\left(\prod_{n=1}^{n_h} G_n(2n)\right)^2\left(\prod_{n=1}^{n_h-1} G_u(2n+1)\right)^4 \qquad [3.a]$$

In this expression, W(2n) is the number of ways of distributing A and B atoms on the m=2n lattice points in the ensemble with the prescribed probability distributions x(i;2n) and is written as

$$W(2n) \equiv \frac{N!}{\prod_i (Nx(i;2n)!)} \qquad [3.b]$$

where N is the number of lattice points in a plane parallel to the IPB. Since the number of systems in an ensemble drops out from the formulation, we did not write it explicitly in eqs. [3]. $G_n(2n)$ is the correlation correction factor for an intra-plane bond at 2n, with the probability $y_n(ij;2n)$, and has the form

$$G_n(2n) \equiv \frac{\prod_i (Nx(i;2n)!) \prod_j (Nx(j;2n)!)}{\prod_{i\,j} (Ny_n(ij;2n)!)\, N!} \qquad [3.c]$$

$G_u(2n+1)$ is the corresponding factor for an inter-plane bond at 2n+1, with $y_u(ij;2n+1)$:

$$G_u(2n+1) \equiv \frac{\prod_i (Nx(i;2n)!) \prod_j (Nx(j;2n+2)!)}{\prod_{i\,j} (Ny_u(ij;2n+1)!) N!} \qquad [3.d]$$

In writing [3.a], the powers 2 and 4 are the multiplicity of the corresponding bonds. In the last factor in [3.a] for the product over G_u the factor for $n=n_h$ factor does not appear because of the end cut off.

The energy of the film is written, using the pair-wise energies $\varepsilon(ij)$, as

$$\frac{E}{N} = 2\sum_{n=1}^{n_h}\left(\sum_{i\,j}\varepsilon(ij)y_n(ij;2n)\right) + 4\sum_{n=1}^{n_h-1}\left(\sum_{i\,j}\varepsilon(ij)y_u(ij;2n+1)\right) \qquad [4]$$

As is usually the case when there are no vacancies, the controlling energy combination is the effective potential ε defined by $4\varepsilon \equiv 2\varepsilon(12) - \varepsilon(11) - \varepsilon(22) > 0$. This is positive when the system is phase-separating as in the present case.

Using the entropy in [3], the energy in [4], and the constraint terms with Lagrange multipliers, we construct the free energy. Minimizing it with respect to individual $y_n(ij;2n)$ and $y_u(ij;2n+1)$, we obtain the following basic equations. We use $\beta = 1/k_BT$. The first group is for y_n's.

$$y_n(ij;2) = \exp(\beta\lambda(2) - \beta\varepsilon(ij)) \times (x(i;2)x(j;2))^{5/6} \exp(2\kappa(i;2) + 2\kappa(j;2)) \qquad [5.a]$$

$$y_n(ij;2n) = \exp(\beta\lambda(2n) - \beta\varepsilon(ij)) \times (x(i;2n)x(j;2n))^{11/12} \exp(2\kappa(i;2n) + 2\kappa(j;2n))$$

$$\text{for } n=2 \text{ to } n_h\text{-}1 \qquad [5.b]$$

$$y_n(ij;2n_h) = \exp(\beta\lambda(2n_h) - \beta\varepsilon(ij)) \times (x(i;2n_h)x(j;2n_h))^{5/6} \exp(2\kappa(i;2n_h) + 2\kappa(j;2n_h)) \quad [5.c]$$

The second group is for y_u's.

$$y_u(ij;3) = \exp(\beta\lambda(3) - \beta\varepsilon(ij)) \times (x(i;2)x(j;4))^{11/12} \exp(-2\kappa(i;2) - \kappa(j;4) - \gamma(j;4)) \quad [6.a]$$

$$y_u(ij;2n+1) = \exp(\beta\lambda(2n+1) - \beta\varepsilon(ij)) \times (x(i;2n)x(j;2n+2))^{11/12}$$

$$\times \exp(-\kappa(i;2n) - \kappa(j;2n+2) + \gamma(i;2n) - \gamma(j;2n+2)) \text{ for } n = 2 \text{ to } n_h\text{-}2 \quad [6.b]$$

$$y_u(ij;2n_h - 1) = \exp(\beta\lambda(2n_h - 1) - \beta\varepsilon(ij)) \times (x(i;2n-2)x(j;2n))^{11/12}$$

$$\times \exp(-\kappa(i;2n_h - 2) + \gamma(i;2n_h - 2) - 2\kappa(j;2n_h)) \quad [6.c]$$

In both groups, (a) and (c) are on the surfaces and (b) is for the interior. These equations can be interpreted intuitively. The λ factor is for the normalization of each y. The $\beta\varepsilon$ part is the Boltzmann factor. Then comes the product of the two x's on the two ends of the bond. The power of the x product depends on the coefficients of the entropy expression. γ is the Lagrange multiplier for [1.a] among y_u's, and κ is for [1.b], [2.a] and [2.b] among y_n's and y_u's.

We solve y's and the Lagrange multipliers from the equations in [5] and [6] together with the constraints in [1], [2] and the normalization conditions. These are a set of non-linear algebraic equations, and can be solved numerically using the Natural Iteration Method (NIM) (9). The NIM is slower than the Newton-Rathson method if the latter can be formulated, but has the advantage that no further transformations are needed after [5] and [6], and also that the guaranteed convergence was proved. Since we are working with the symmetric case, we choose the initial state of the iteration to satisfy the required symmetry. For example, we may start with a relatively simple distribution:

$$\begin{aligned} x(1;2n) &= 0.8 \quad \text{for } n = 1 \text{ to } n_1 \\ x(1;2n) &= 0.2 \quad \text{for } n = n_1+1 \text{ to } n_h \end{aligned} \quad [7]$$

where $n_1 = n_h/2$. Convergence of the iteration is fast.

RESULTS

The critical point of the miscibility gap in a bulk system of fcc calculated based on the pair approximation is $k_BT_c/\varepsilon = 10.970$. In Figure 2 we plot the density profile of A atoms (i=1) for six different thicknesses for $k_BT/\varepsilon = 8.0$ ($< k_BT_c/\varepsilon$). The abscissa n counts the lattice planes, while the ordinate is x(1; 2n) at the coordinate m = 2n. At the IBP center, x(1; 2n) is equal to 0.5, which occurs at the *interstitial center* m = −1, which lies between n = −1 and n = 0 planes.

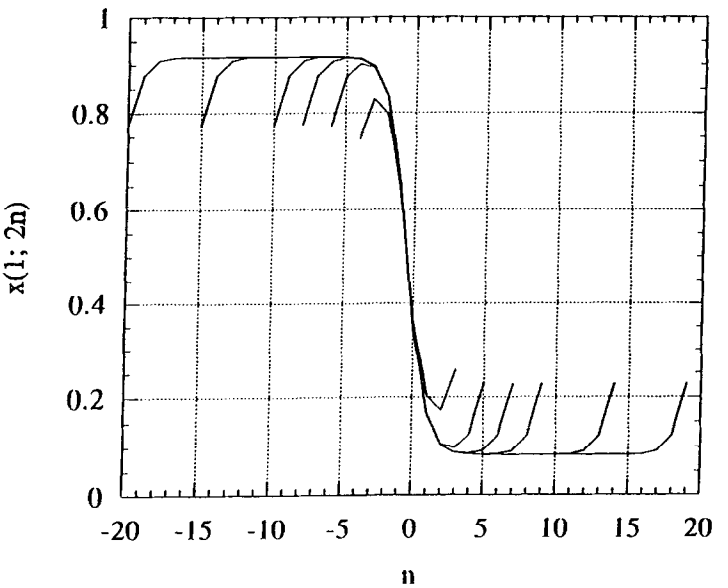

Figure 2. The composition profile x(1; 2n) of A atoms for k_BT/ε=8.0 for six different thicknesses, n_h=8, 12, 16, 20, 30 and 40. The abscissa n counts the lattice plane, and 2n in x(1; 2n) is the coordinate of the plane identified by n.

Figure 2 shows the following features. (i) In relatively thick films the inside part of x(1; 2n) is practically equal to the bulk 3-D value. (ii) The 3 lattice planes near the surface and the 3 planes near the IBP center bend down. (iii) The surface of the film is the 2-D plane, and this influences the x(1; 2n) value. Since the x(1; 2n) for a 2-D plane is smaller than the bulk 3-D value for this temperature, the surface segregation is smaller so that x(1; 2n) bends down near the surface on the left-hand side. We see the reverse case in Figure 3. (iv) When the film thickness is 2×6 and smaller, the profile never takes the 3-D value. (v) For this temperature, $n_h \leq 6$ cases are not plotted in Figure 2 since the film does not phase separate and x(1; 2n) = 0.5.

In Figure 3 we plot profiles for different temperatures for four thicknesses. The n_h=20 curves in (a) show that the end effect and the IPB center effect are felt deeper for higher temperatures, *i.e.* for inner curves. Curves in Figure 3 indicate that the profile becomes flatter as the temperature increases. Comparison of (d) with the rest of Figure 3 indicates that the segregation near the surface reverses in (d). This reversal is due to the anchoring of the surface density at or near the value for the 2-D surface plane. The temperature at which the curve becomes flat, *i.e.* x(1; 2n) = 0.5 for all n, is the critical temperature T_c. T_c thus determined are plotted with circles in the lower curve in Figure 4 against the film thickness n_h. The plots indicate how the curve asymptotically approaches the bulk value k_BT_c/ε = 10.97 as the thickness increases. We compare this result with the periodic layer case, Figure 5 of Paper I, which is plotted with squares in Figure 4.

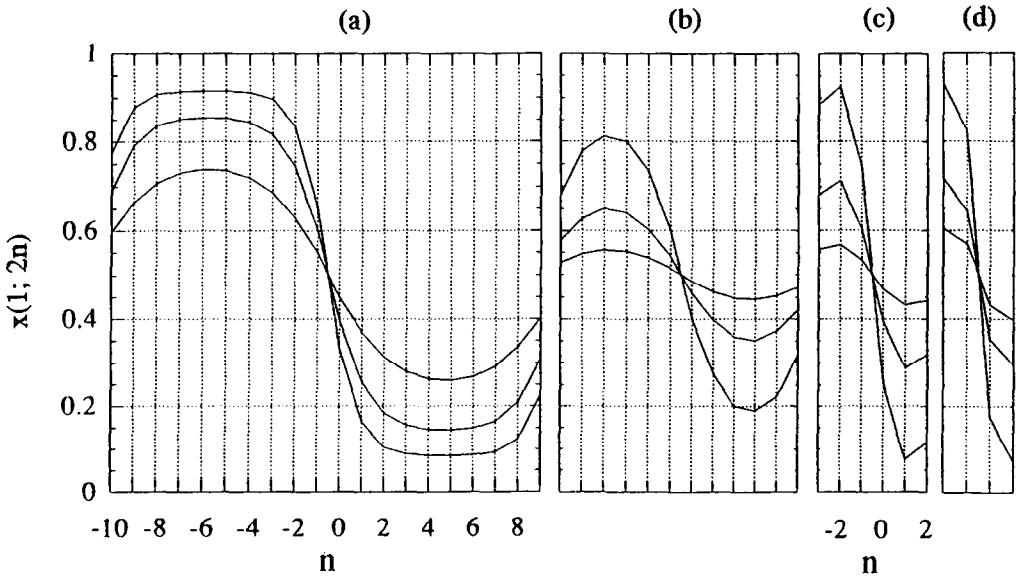

Figure 3. The composition profile x(1; 2n) for different thicknesses n_h. (a) is for n_h=20, and k_BT/ε for the curves are from outside to inside 8, 9 and 10. (b) is for n_h=12, for k_BT/ε of 9.0, 9.8 and 9.97. (c) is for n_h=6, for k_BT/ε of 6.0, 7.5 and 7.8. (d) is for n_h=4, for k_BT/ε of 4.0, 5.0 and 5.17.

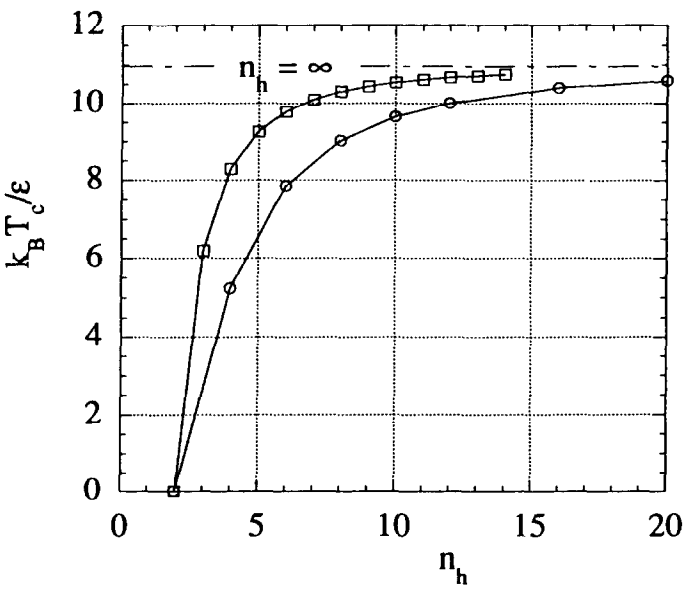

Figure 4. The lower curve with circles is the phase-separating critical point k_BT_c/ε plotted against the film thickness n_h in the present case. The upper curve with squares is the replot of Figure 5 in Paper I for the periodic layer structure.

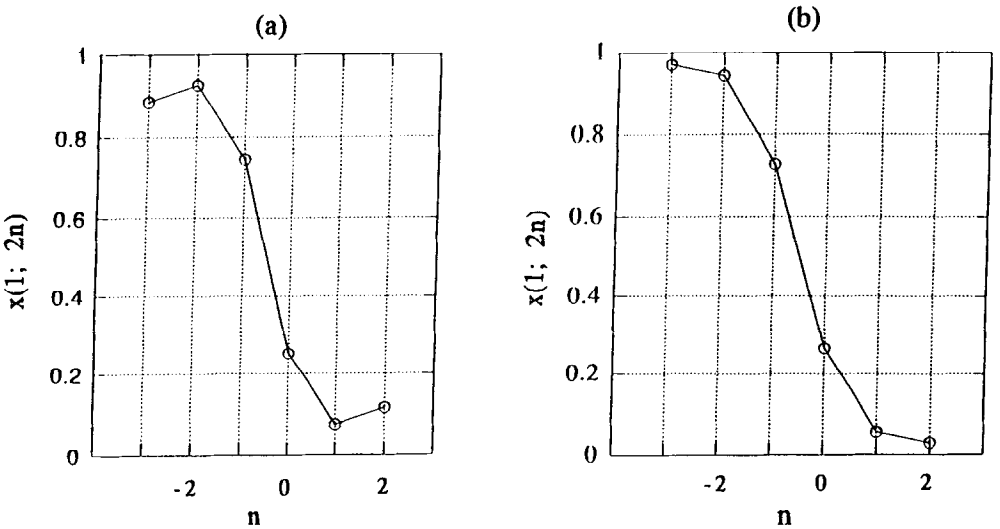

Figure 5. Comparison of the composition profile x(1; 2n) for (a) the film and (b) the periodic layer cases. $k_BT/\varepsilon=6$ and the thickness is 6 lattice planes.

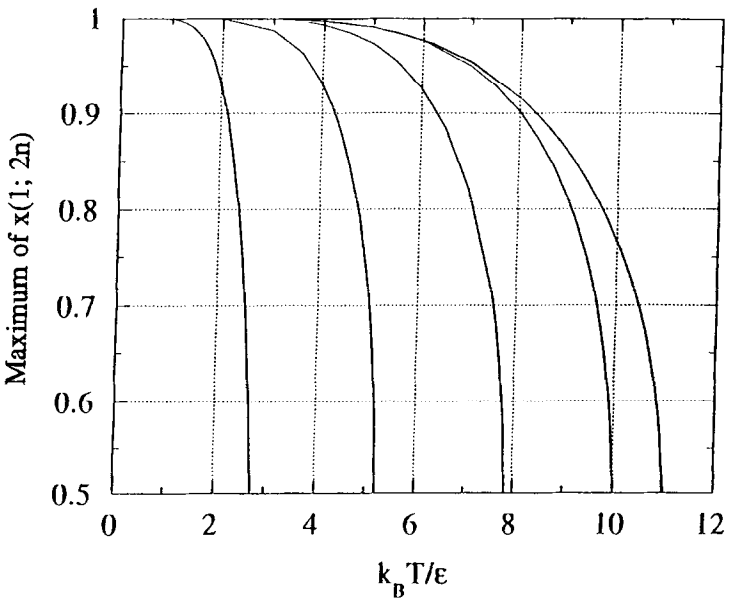

Figure 6. The "phase diagram" of the film, *i.e.* the maximum x(1; 2n) for the designated thickness and k_BT/ε. Curves are, from right to left: (a) the bulk phase diagram for fcc; (b) for thickness $n_h=12$; (c) $n_h=6$; (d) $n_h=4$; and (e) the bulk 2-D square lattice. The bulk curves are for comparison.

Another comparison is made in Figure 5. (a) is a replot of Figure 3 (c) for n_h=6 for the temperature k_BT/ε=6, and (b) is the corresponding case for the periodic layer structure. The main difference is the effect of the free surfaces, which exists in (a) but not in (b). In the periodic layer case, the maximum value of x(1; 2n) occurs at the center of the high region as is seen in Figure 5(b). We plotted this value against temperature for different thicknesses in Paper I, Figure 4 (reproduced in Figure 7 in this paper), which can be regarded as the "phase diagram" of the layer structure. For the film case, the maximum value of x(1; 2n) appears either at the surface as in Figure 3(d), or inside as in other cases of Figure 3. We plot these maximum values for different film thicknesses against temperature in Figure 6, which we may interpret as the "phase diagram" of the film structure of each thickness. For comparison, we also plot the bulk 3-D fcc curve in (a), and the bulk 2-D square lattice values in (e). The latter is the structure of the (100) surface of fcc.

SUMMARY AND DISCUSSION

We study the structure of thin films of a binary alloy of phase-separating interaction containing an IPB in it. The model is an A-B alloy of the equal atomic composition on the fcc lattice with no vacancies. The problem is identical with that of the Ising model. The film is placed along the [100] orientation. We calculate the composition profile and the pair correlations using the pair approximation of the Cluster Variation Method.

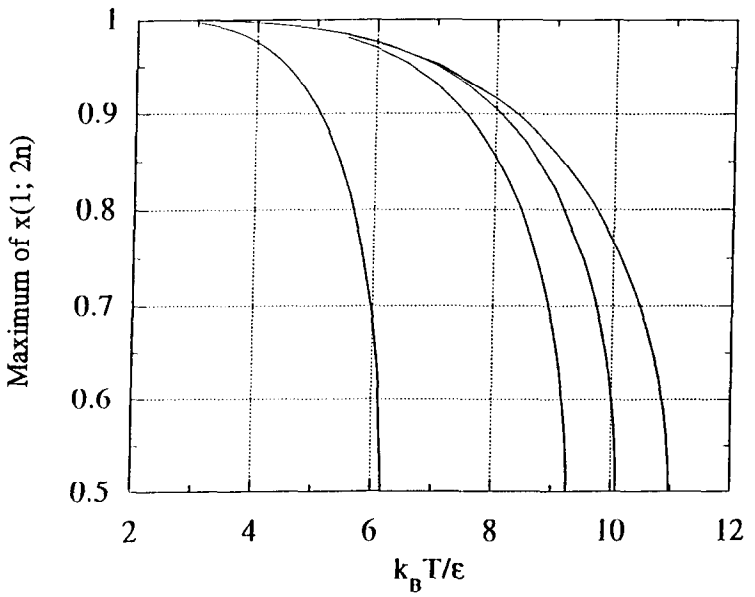

Figure 7. The "phase diagram" of the periodic layer case, to be compared with Figure 6. Reproduction of Figure 4 in Paper I. The curves are the plots of the maximum values of the local composition. From right to left, for the thicknesses, *i.e.* the number of planes in a half period, of (a) ∞; (b) 7; (c) 5; and (d) 3.

The composition profiles of A atoms are plotted as functions of temperature and thickness, in Figures 2 and 3. At the surface, the composition is influenced by the square lattice properties of the (100) surface plane. The depth of the surface effect is about 3 lattice planes at low temperatures, and is somewhat similar as the IPB width. The critical temperature T_c of phase separation is calculated for each thickness as plotted in Figure 4. When we compare the profiles of the present thin film and the corresponding periodic layer structure (Figure 5), we clearly see the effect of the free surface. The maximum local density of A for a fixed film thickness varies between 1.0 and 0.5. Figure 5 plots the maximum local density of A against temperature for selected thicknesses. We can regard this plot as the "phase diagram" for a film.

Two comments on the method are in order. The first is concerning how reliable the pair approximation results are. The numerical results are somewhat altered when larger size basic clusters are used in the formulation. However, our previous experience shows that the qualitative features remain the same in the phase-separating system. The second point is about the Monte Carlo simulation. Since the film is of finite thickness, M. C. is a viable technique, and can lead to values close to rigorous results, if sufficient time and labor are spent. The advantage of the pair approximation is that it is much faster and many cases can be studied in a short time.

ACKNOWLEDGMENT

This project was supported by NSF under grant number DMR-9311898 (L.-Q.C.), and by ARPA under the NIST program on Modeling of Microstructure Evolution in Advanced Alloys (RK).

REFERENCES

1. R. Kikuchi and L.-Q. Chen, Nanostruct. Mater. 5, 257 (1995).
2. R. Kikuchi, L.-Q. Chen and A. Beldjenna, Nanostruct. Mater. 5, 269 (1995).
3. R. Kikuchi, Phys. Rev. 81, 988 (1951).
4. R. Kikuchi and A. Beldjenna, Physica A 182, 617 (1992).
5. R. Kikuchi and L.-Q. Chen, *Computer Aided Innovation of New Materials II*, eds. M. Doyama, J. Kiraha, M. Tanaka and R. Yamamoto, Elsevier Science Publishers B.V., p. 735 (1993).
6. A. Díaz-Ortiz, F. Aguilera-Granja and J.L. Morán-López, *New Trends in Magnetic Materials and Their Applications*, eds. J.L. Morán-López and J.M. Sanchez, Plenum Press, NY, p. 131 (1994).
7. R. Kikuchi and J.W. Cahn, Phys. Chem. Solids 23, 137 (1962).
8. R. Kikuchi, Prog. Theor. Phys., Suppl., No. 115, p.1 (1994).
9. R. Kikuchi, J. Chem. Phys. 60, 1071 (1974).